Journal of Engineering and Technology for Industrial Applications

ITEGAM-JETIA

Manaus, v.11 n.51, p. 227-235. January/February., 2025.
DOI: https://doi.org/10.5935/jetia.v11i51.1487

ISSN ONLINE: 2447-0228

RESEARCH ARTICLE OPEN ACCESS

NUMERICAL INVESTIGATION OF TWO-PHASE THERMAL-HYDRAULIC, CHARACTERISTIC AND ENTROPY GENERATION OF WATER-BASED AL_2O_3-CU HYBRID NANOFLUIDS IN MICROCHANNEL HEAT SINK

Olabode Thomas Olakoyejo[1], Emmauel Adeyemi[2], SettingsOlayinka Omowunmi Adewumi[3], Sogo Mayokun Abolarin[4], Ibrahim Ademola Fetuga[5], SettingsAdekunle Omolade Adelaja[6]

[1,2,3,5,6] Department of Mechanical Engineering, University of Lagos, Akoka, Lagos, Nigeria;
[4] Department Engineering Sciences, University of the Free State, Bloemfontein, South Africa

[1]http://orcid.org/0000-0001-9942-1339, [2]https://orcid.org/0009-0004-4394-763X, [3] https://orcid.org/0000-0002-3545-6679,
[4]https://orcid.org/0000-0002-1712-5104, [5] https://orcid.org/0000-0002-1943-4234, [6] https://orcid.org/0000-0001-9175-8332

Email: *oolakoyejo@unilag.edu.ng, 170404510@live.unilag.edu.ng, oadewumi@unilag.edu.ng, AbolarinSM@ufs.ac.za, fetugaebraheem@gmail.com, aadelaja@unilag.edu.ng.

ARTICLE INFO

Article History
Received: December 17, 2024
Revised: January 20, 2025
Accepted: January 25, 2025
Published: February 28, 2025

Keywords:
heat sink,
hybrid nanofluid,
Reynolds Number,
Nusselt number,
entropy generation.

ABSTRACT

This study employs numerical simulations to investigate the impact of water-based hybrid nanofluid containing copper-alumina nanoparticles using two-phase Eulerian-Eulerian model and finite volume approach to solve the conjugate heat transfer problem in a three-dimensional microchannel heat sink. The aim is to numerically evaluate the thermal behaviour and performance criteria of the microchannel heat sink using Ansys workbench, while determining the influence of volume concentration and Reynolds number (*Re*) on Nusselt number, friction factor and entropy generation. Generally, the heat sink consists of a silicon cylindrical structure block forming a microchannel heat sink with an internal heat generation of 10^8 W/m$^{3.}$ The study involves varying the Reynolds number across a range of 100 to 500. This variation applies to distinct volume concentrations of alumina-copper nanoparticles, specifically alternating between 0.25%, 0.50%, and 0.75% for a volume fraction of 1%. Additionally, the volume concentration was further adjusted within the range of 1% to 4%. The verification of the numerical models shows excellent agreement with literature. The results reveal that higher relative concentrations of copper nanoparticles lead to improved thermal enhancement of the hybridized nanofluid. An increase in both the Reynolds number (*Re*) and the concentration of Cu in the hybrid nanofluids caused a reduction in total entropy generation and thermal entropy generation. For *Re* = 500 and volume concentration of 4% in relation to the base fluid, the friction factor increases by less than 1%, the Nusselt number experienced an increase of 8.73% while the total entropy generation rate experiences 4.9% increase. At a concentration of 4.0% volume, the maximum figure of merit corresponds to a Reynolds number of 100 with 9.10% shift from 1.0% volume of hybrid nanofluid.

I. INTRODUCTION

Non-uniform heat generation is a prevalent occurrence in electronic equipment Feng et al [1]. To relieve the thermal load on electrical gadgets, this heat creation necessitates an optimized and clear channel with cooling fluid. Over the years, engineers and scientists have applied different methods from single phase, two phase to multiphase as an efficient way to remove the heat dissipated in the system, but due to the limitation of low thermal conductivity, Choi and Eastman [2] engineered a new fluid through the incorporation of metallic nanoparticles into heat transfer fluids, resulting in a suspension. This innovation is what is known as

Nanofluid (NF) today and circulated in thermal systems as alternative to conventional fluids.

II. THEORETICAL REFERENCE

The study of nanofluids and heat removal continue to grow gradually from homogeneous single phase to two-phase and multiphase. For single phase flow, Olakoyejo et al [3] investigated and optimized cylindrical micro-cooling channels with variable cross - section using the constructal theory. Their results showed that there were optimal inlet and outlet diameters that enhanced the performance of the micro-cooling channel. Also, in order to observe the heat transmission and drop in pressure of a system, Kumar and Sarkar [4] considered a 2-phase model to replicate the flow of forced convection in a heat sink (microchannel), using water/Al_2O_3 NF and Al_2O_3-MWCNT hybrid NF. The homogeneous and heterogeneous models display a good relationship with experiment results.

Hybrid nanofluids are group of fluids that comprise two or more types of nanoparticles and base fluids. They have gained significant acceptance recently due to their potential to alter the transfer of heat performance in two-phase flow systems, such as condensation and boiling. The circulation of hybrid nanofluids in thermal systems has shown promising results in various industrial applications, including power generation and refrigeration. This results in a unique set of properties that are not present in either the individual nanoparticles or the base fluid alone. This innovation has attracted significant attention in recent years due to its potential to enhance transfer of heat and improve the performance of cooling systems. Recently, Dey and Sahu [5] studied and reviewed the advantages of two-phase heat transfer and the potential benefits of using NFs in various two-phase heat transfer applications. According to the research, the convective transfer of heat coefficient is notably more with two-phase transfer of heat in comparison with alternative modes of transfer of heat.

Various studies have examined the usage of hybrid NFs for improving the transfer of heat performance in two-phase flow systems. In literature,transfer of heat and pressure drop are affected by circulating hybrid nanofluids through and or around heat sink using two-phase model [6 - 9]. Similarly,entropy generation has also been influenced whenever nanofluids and hybrid NF are circulated in thermal systems [10], [12]. Nimmagadda and Venkatasubbaiah [13] investigates the convection flow (laminar – forced) of different nanofluids in a micro-channel of rectangular shape with low *Re* (10 - 50). The results indicate that nanofluids with less particle diameter are preferred for heat transfer enhancement, while raising the concentration of nanofluids enhances the *Nu* and improves thermal conductivity, the solid/liqud interface region temperature increases with increase in length of channel.

Alfaryjat et al [14] numerically investigated the heat transfer enhancement of hexagonal heat sink microchannel using Alumina/H_2O, CuO/H_2O, SiO_2/H_2O and ZnO//H_2O nanofluid. The authors compared the performance of the nanofluids while varying volume fractions from (0% - 4%) at *Re* 100-1000. Their results indicate that Alumina/H_2O is favourable due to its minimal dimensionless temperature, coupled with the highest heat transfer coefficient (*h*). On the other hand, SiO_2/H_2O exhibits the greatest pressure drop, while pure water experiences the least..

Balaji et al [15] analyzed how functionalized Graphene Nanoplatelets (f-GnP) suspended in distilled water affected convective heat transfer. The study found that f-GnP-based nanofluids having concentration between 0% to 0.2% could improve convective h and Nu by 71% and 60% respectively at mass flow rate of (5g/s - 30g/s). The researchers suggested that these nanofluids could replace concentional cooling fluids to enhance electronic chips' performance via improved transfer of heat and thermal conductivity.

Krishna et al [16] examined the pressure drop and transfer of heat capacity MWCNT-CuO/water-based hybrid nanofluid in MCHS with circular cross section with *Re* ranging from 500-2000. The study shows that drop in pressure was less with hybrid-nanofluids in comparison with CuO/water nanofluids and 3% maximum enhancement of Nu was found for the hybrid NF.

Vinoth and Sachuthananthan [17] compared the performance of pentagonal and triangular oblique finned microchannel heat sinks, using different nanofluids (CuO/H_2O, Al_2O_3/H_2O and Al_2O_3-CuO/H_2O) at varying mass flow rate of 0.1-0.5 litres per minute. The pentagonal mini-channel performed better, especially with hybrid nanofluid due to secondary flow, and had higher Performance Evaluation Criterion than the triangular heat mini-channel.

The use of hybrid nanofluids has shown promising results in enhancing the transfer of heat performance in two phase flow systems. The studies have explored the potential of hybrid nanofluids for various industrial applications, including power generation, refrigeration, and heat exchangers.

The present research is driven by the existing gap in numerical investigations utilising the two-phase Eulerian method within the ANSYS – Fluent framework. The objective is to comprehensively examine the thermal-hydraulic behavior of a hybrid NF in a multi-scale cylindrical channel. This investigation is also inspired by the preceding works conducted by Muzychka [18] and Omoshin et al [19], which shed light on the impact of smaller microchannels on the overall thermal efficiency of systems and effect of nanoparticles hybridization, respectively. This work introduces arrays of smaller microchannels to cylindrical channel in order to improve its performance and design was further streamlined into a sector multiscale elemental volume.

III. METHODOLOGY

II.1 PROBLEM FORMULATION

Figure 1(a) depicts the physical configuration of the model considered in this study. The model is considered to be micro-electronic component that comprises of an array of sector cooling channels with fixed global volume, *V* and length *L*. The entire solid material experiences s an internal heat of 10^8 W/m^3, which is denoted as q'''. Fig. 1(b) shows an elemental volume containing a sector and interstitial circular cooling while and Table 1 summarizes the dimensions of the elemental volume used for this study. Forced convection is employed to remove heat from the system, where coolant, water-(Al_2O_3-Cu) hybrid nanofluid with 0%, 1%, 2%, 3% and 4% nanoparticle concentration is circulated into the cooling channels at varying inlet Reynold numbers over the channel length *L*. The analysis assumes a uniform heat distribution within the channel, given that the surrounding element is used in the analysis. The fluid was considered to be two-phase Eulerian fluid with particle diameter of 10^{-8} and interfacial area of ia-particle. The fluid was circulated through the six-patterned holes and centered circular channel to remove heat from the solid body at every hotspot.

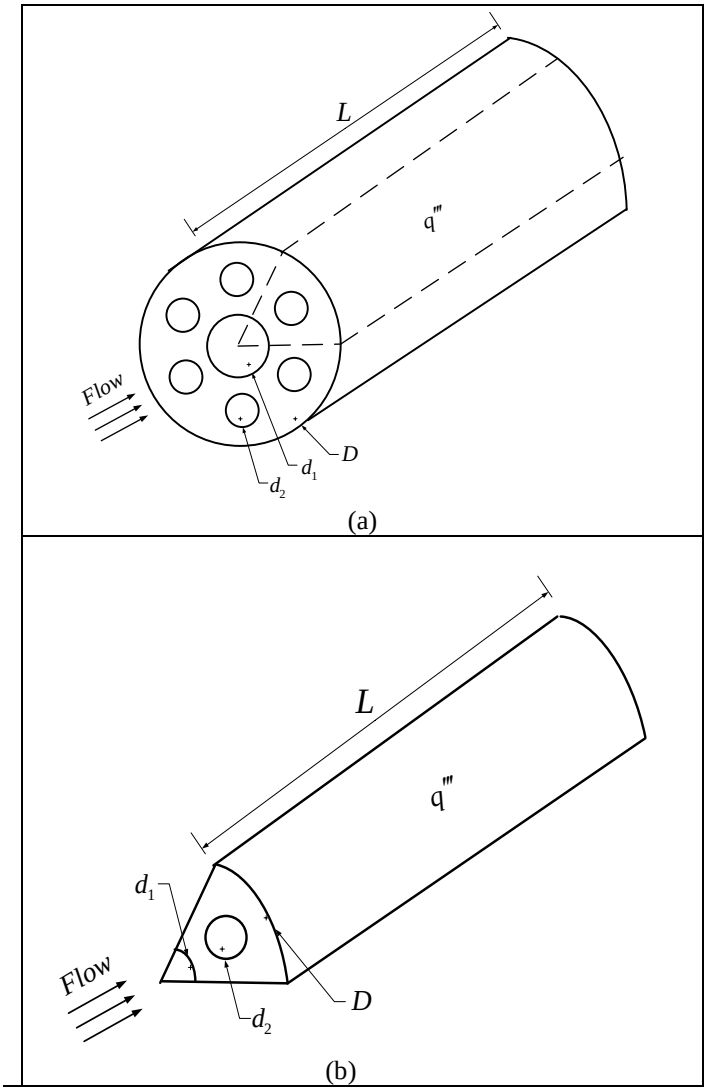

Figure 1: The three-dimensional (a) global and elemental volume with circular and (b) sector channels
Source: Authors, (2025).

D (μm)	d_1 (μm)	d_2 (μm)	L (μm)
1200	400	200	10000

In Figure. 1(b), the elemental volume, is conceptualized to be made up of an elemental channel with sector channel diameters d_1 and interstitial channel circular d_2:

II.2 GOVERNING EQUATIONS AND BOUNDARY CONDITIONS

A. Governing equations

The mathematical (continuity, momentum, energy) equations that describe the behavior of this numerical study are formulated with the assumption that the flow is two phase using hybrid-nanofluid.

Continuity equation

$$\nabla \cdot (\alpha_1 \rho_1 \vec{u}_1) = 0 \tag{1a}$$

Solid phase:

$$\nabla \cdot (\alpha_2 \rho_2 \vec{u}_2) = 0 \tag{1b}$$

$$\nabla \cdot (\alpha_3 \rho_3 \vec{u}_3) = 0 \tag{1c}$$

whereρ, α, $\vec{u}$ are the density, volume concentration, and velocity vector while subscripts 1, 2, 3 represents primary phase (water), secondary phase (alumina nanoparticles), secondary phase (copper nanoparticles) respectively.

$$\alpha_1 + \alpha_2 + \alpha_3 = 1 \tag{1d}$$

Momentum equation

Liquid phase:

$$\nabla \cdot (\alpha_1 \rho_1 \vec{u}_1) = -\alpha_1 \nabla p + \nabla \cdot \left[\alpha_1 \mu_1 (\nabla \vec{u}_1 + \nabla \vec{u}_1^{\,T}) \right] + F_d + F_{MV} \tag{2}$$

Solid phase:

$$\nabla \cdot (\alpha_2 \rho_2 \vec{u}_2) = -\alpha_2 \nabla p + \nabla \cdot \left[\alpha_2 \mu_2 (\nabla \vec{u}_2 + \nabla \vec{u}_2^{\,T}) \right] - F_d - F_{MV} + F_{col} \tag{3}$$

$$\nabla \cdot (\alpha_3 \rho_3 \vec{u}_3) = -\alpha_3 \nabla p + \nabla \cdot \left[\alpha_3 \mu_3 (\nabla \vec{u}_3 + \nabla \vec{u}_3^{\,T}) \right] - F_d - F_{MV} + F_{col} \tag{4}$$

where P, μ_2, F_d, F_{MV}, F_d F_{MV} and F_{col} are the the pressure, dynamic viscosity, drag, virtual mass, and particle-to-particle interaction forces, respectively. However, according to Kalteh et al. [20], the virtual mass and particle to particle interaction force have an insignificant effect on heat transfer characteristics (Nusselt number). Hence, only the drag force and convective heat transfer between the primary and secondary phases are considered. The particle-to-particle heat transfer is neglected, and the gravitational and the lift forces attributable to the small size of the particles are also ignored.

The drag force between the primary phase and each secondary phase (alumina and copper particle) is calculated as

$$F_d = -\beta (\vec{u}_1 + \vec{u}_P) \tag{5}$$

$$\beta = \frac{3}{4} C_d \frac{\alpha_1 \alpha_p}{\varphi_p d_p} \rho_1 \left| \vec{u}_1 + \vec{u}_P \right| \alpha_1^{-2.65} \tag{6}$$

where C_d is the drag coefficient.

Energy equation

$$\nabla \cdot (\alpha_1 \rho_1 C_{p_1} T_1 \vec{u}_1) = \nabla \cdot (\alpha_1 K_1 \nabla T_1) - Q_h \tag{8a}$$

$$\nabla \cdot (\alpha_2 \rho_2 C_{p_2} T_2 \vec{u}_2) = \nabla \cdot (\alpha_2 K_2 \nabla T_2) + Q_h \tag{8b}$$

$$\nabla \cdot (\alpha_3 \rho_3 C_{p_3} T_3 \vec{u}_3) = \nabla \cdot (\alpha_3 K_3 \nabla T_3) + Q_h \tag{8c}$$

where *T, K, C_p,* are the temperature, thermal conductivity specific heat capacity. Q_h is the volumetric energy transfer rate between the primary and each secondary phase, and it is expressed as

$$Q_{pq} = h_{p,1}\frac{6\alpha_p}{d_p}(T_P - T_1) \quad (9)$$

where *h, d,* and subscript *p* are the heat transfer coefficient, diameter, and particulate, respectively

B. Boundary conditions

The expression for the heat flux across the solid-liquid interfaces is given as:

$$k_s\frac{\partial T}{\partial n}\bigg| = k_{nf}\frac{\partial T}{\partial n}\bigg| \quad (10)$$

The fluid velocities close to the channel walls are expressed as:

$$\dot{v} = 0 \quad (11)$$

The inlets conditions are given as:

$$T = T_{in} \quad (12)$$

$$u_f = u_{in} \quad (13)$$

Eq. (24) is uniform axial velocity for both base fluid and particulate phases at bottom channel while the outlet condition is ambient outflow condition.

The solid boundary given as:

$$\nabla T = 0 \quad (14)$$

II.3 PERFORMANCE CRITERIA

The criteria that are utilized to determine the performance characteristics of the cooling channel are now discussed.

II.3.1 NUSSELT NUMBER

Average Nusselt number (*Nu*) is one of the measures of heat transfer performance for this study and this was determined by taking the value obtained by multiplying transfer of heat coefficient and the hydraulic diameter divided by the thermal conductivity.

$$Nu = \frac{q'''D_hL}{k_f\left(T_w - T_{in}\right)} \quad (15)$$

where *kf,* is the thermal conductivity of the liquid [4,5]. and T_w is the area-weighted average wall temperature. T_w is the wall temperature at the center of the heated base and D_h average hydraulic diameter.

II.3.2 FRICTION FACTOR

The calculation of the friction factor *f,* which is a measure of microchannel performance characteristics, was carried out and presented as follows:

$$f = \frac{2\Delta pD_h}{\rho u_{nf}^2 L} \quad (16)$$

II.3.3 ENTROPY GENERATION

This study also investigated the practical importance of total volumetric entropy generation rate ($S'''_{g\text{-}total}$), which is a measure of the inability to reverse a process. This criterion was conveyed as shown by Alfaryjat et al [21]

$$\dot{S}_{g-total} = \dot{S}_{g-th} + \dot{S}_{g-fr} \quad (17)$$

where the thermal entropy generation ($\dot{S}_{g-th}$) and the friction entropy generation ($\dot{S}_{g-fr}$) were determined as expressed individually as:

$$\dot{S}'''_{g-th} = \frac{k_{nf}}{T^2}\left(\left(\frac{\partial T}{\partial x}\right)^2 + \left(\frac{\partial T}{\partial y}\right)^2 + \left(\frac{\partial T}{\partial z}\right)^2\right) \quad (18)$$

$$\dot{S}'''_{g-th} = \frac{\mu_{nf}}{T}\left\{\begin{array}{l} 2\left(\left(\frac{\partial u}{\partial x}\right)^2 + \left(\frac{\partial v}{\partial y}\right)^2 + \left(\frac{\partial w}{\partial z}\right)^2\right) \\ +\left(\frac{\partial v}{\partial x} + \frac{\partial u}{\partial y}\right)^2 + \left(\frac{\partial w}{\partial x} + \frac{\partial u}{\partial z}\right)^2 + \left(\frac{\partial v}{\partial z} + \frac{\partial w}{\partial y}\right)^2 \end{array}\right\} \quad (19)$$

II.3.2 FIGURE OF MERIT

In order to assess the trade-off between increasing power required for pumping and the rate of heat transfer improvements, the Figure of Merit (FOM) is utilized to evaluate the overall performance of each of the suggested designs. FOM is give according to Ali et al [22].

$$FOM = \left(\frac{Nu_{nf}}{Nu_{bf}}\right) \div \left(\frac{f_{nf}}{f_{bf}}\right)^{\frac{1}{3}} \quad (20)$$

III COMPUTATIONAL PROCEDURE

III.1 NUMERICAL TECHNIQUE

This CFD study was conducted using ANSYS Fluent software. A phase coupled SIMPLE approach was utilized for pressure/velocity couple with the pressure, momentum, volume fraction, granular temperature and the energy equations solved using the second-order upwind technique. A multiphase approach with an homogeneous Eulerian model was assumed while the number of Eulerian phase and volume fraction parameters formulation were set to two and implicit respectively. The primary phase used was water-liquid and secondary phase was aluminium-oxide and copper hybrid nanofluid with syamlal-obrien assumed for the granular viscosity, solids pressure and granular conductivity. The temperature granular model was solved with partial differential equation. For phase interaction, phase 1 was given a drag coefficient of syamlal-obrien and a virtual mass drag of 0.5 with no lift and surface tension coefficient. The phase 2 was given a collision coefficient of 0.9 in the force setup while interfacial area of ia-particle was set for the phases.

III.2 GRID INDEPENDENCE TEST

Different grid tests were performed to ascertain this study's accuracy and the convergence criterion was determined using:

$$\gamma = \frac{\left|(T_{\max})_i - (T_{\max})_{i-1}\right|}{\left|(T_{\max})_i\right|} \leq 10^{-5} \quad (21)$$

Figure. 2. shows the computational mesh of this study. Table 2 outlines grid independence test carried out in this study. The number of elements corresponding to the number of nodes 15715, 60649, 96783 and 270 520 are 80711, 322051, 1458163 respectively. The *i*-1 mesh was chosen because it fulfilled the criterion convergence and a further increment had no influence on the result. The test shows that increasing the number of elements beyond 96873 could not cause a significant change in the maximum temperature. Hence, the mesh with 96,783 nodes and 510,569 elements was used for this computational study

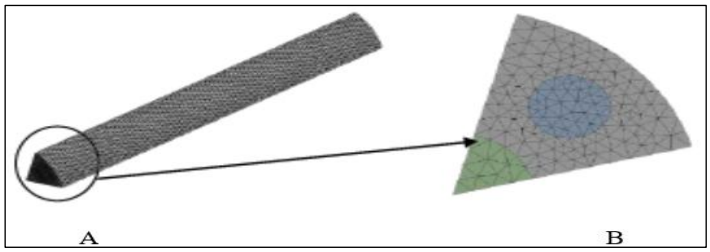

Figure. 2: Computation study mesh
Source: Authors, (2025).

Table 2: The grid independence study for CFD study

L = 0.01 m, R = 600 µm, D_c = 200 µm, R_s = 200 µm, Re = 100 and $\varnothing$ = 1%			
Number of Nodes	Number of Elements	T_{max} (K)	γ
15,715	80,711	301.1814	-
60,649	322,051	302.2358	0.0034890
96,783	510,569	302.2318	0.00001323
270,520	1,458,163	302.2302	0.0000005294

III.3 NUMERICAL CODE VALIDATION

Figure 3 presents a validation of the numerical model, comparing it with previous experiments conducted by Azizi et al. [23]. These experiments utilized a circular microchannel with a heat flux set at 35 kW/m² and *Re* between 280 and 780. The observed trends align closely, with a mean average deviation of less than 10%.

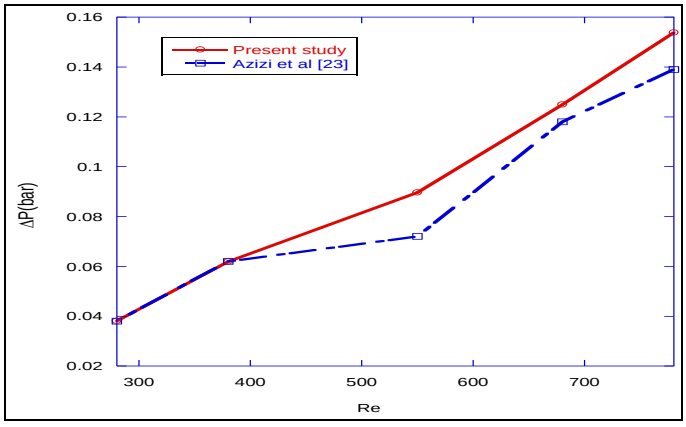

Figure 3: Validation of present study with Azizi et al [23]
Source: Authors, (2025).

IV. RESULTS AND DISCUSSIONS

This section outlines the findings of this study's investigation on the impact of hybrid NFs on the friction factor, entropy generation and avergae Nusselt numbers *Nu* of both inlet configurations. The study involved testing various combinations of hybrid nanoparticles at nanoparticle concentrations ranging from zero (pure water) to 4.0% volume concentration, while the *Re* was varied between 100 and 500.

IV.1 INFLUENCE OF NANOPARTICLE CONCENTATION (*Φ*) AND REYNOLDS NUMBERON NUSSELT NUMBER

In Figure 4, the relationship between Reynolds numbers (*Re*) and avergae Nusselt numbers (*Nu*) is shown. As *Re* increases, there is a clear upward trend in *Nu*, consistent with observations made by Zheng et al. [24]. The study also evaluates the heat transfer effects of differing concentrations of Al_2O_3 and *Cu* within hybrid nanofluids.

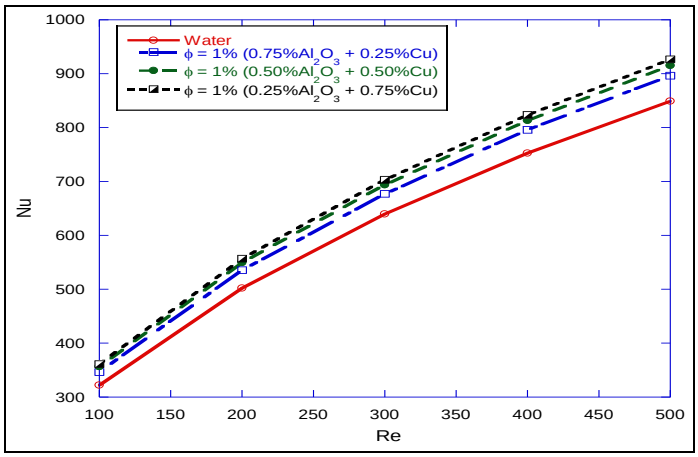

Figure 4: Effect of Reynolds number on average Nusselt number at fixed hybrid nano particle concentration
Source: Authors, (2025).

Results demonstrate that Cu, at higher concentrations, tends to perform better than Al_2O_3. In scenarios where Al_2O_3 and Cu are present in equal concentrations, their performance surpasses that of both pure water and Al_2O_3 alone, suggesting significant improvements in heat transfer when Cu is incorporated into hybrid nanofluids. At a *Re* of 100, without any nanofluid particles, the *Nu* stands at 321.85. This figure climbs to 346.34 when the concentration of Cu in the hybrid nanofluid reaches 0.25%. As the Cu concentration increases to 0.50% and 0.75%, the *Nu* further ascends to 356.45 and 360.97, respectively. Additionally, at a *Re* of 500, *Nu* values corresponding to Cu concentrations of 0.25%, 0.50%, and 0.75% are 896.65, 915.34, and 926.67, respectively. These findings indicate an enhancement in *Nu* by 10.17% at a *Re* of 100 and by 7.49% at a Re of 500 when Cu concentration is raised from 0.25% to 0.75%.

IV.2 EFFECT OF NANOPARTICLE HYBRIDIZATION ON THE AVERAGE NUSSELT NUMBER

The Nusselt number, expressed non-dimensionally, serves as a crucial indicator for assessing and forecasting the heat transfer efficiency of thermal systems. As depicted in Figure 5, there is a notable rise in the Nusselt number with increases in Reynolds number, Reynolds number which shows similar trends with worked presented by Ataei et al [25].

It is observed that a higher concentration of Cu within the hybrid nanofluids leads to improved thermal performance. Notably, the hybrid nanofluid with 4% Cu concentration exhibits the most significant enhancement in thermal performance.

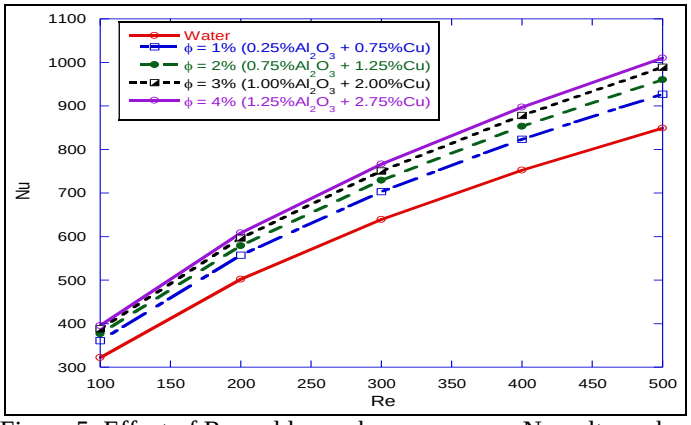

Figure 5: Effect of Reynolds number on average Nusselt number at different hybrid nanoparticle concentration
Source: Authors, (2025).

Furthermore, increasing the proportion of Cu in the Al2O3 mixture results in greater improvements in heat transfer capabilities. Specifically, at a Reynolds number of 100, the Nusselt number progresses from 360.97 to 376.84, 388.10, and finally 395.73 as the Cu concentration increases to 1%, 2%, 3%, and 4%, respectively. At a Reynolds number of 500, the Nusselt numbers associated with Cu concentrations of 1%, 2%, 3%, and 4% are 926.67, 960.43, 989.02, and 1010.1, respectively. This indicates that a rise in Cu concentration from 1% to 4% escalates the Nusselt number by 12.15%, 17.09%, 20.58%, and 22.95% compared to the base fluid, at a Reynolds number of 100.

IV.2 4.3 INFLUENCE OF NANOPARTICLE CONCENTATION (*Φ*) AND REYNOLDS ON FRICTION FACTOR (*f*)

The bar chart in Figure 6 explores the response of hybrid nanofluids to changes in Reynolds number and alumina nanoparticle content. The experiments maintained a constant nanoparticle concentration of 1% while varying the Reynolds number from 100 to 500. The data demonstrate that variations in nanoparticle concentration have a negligible impact on the friction factor.

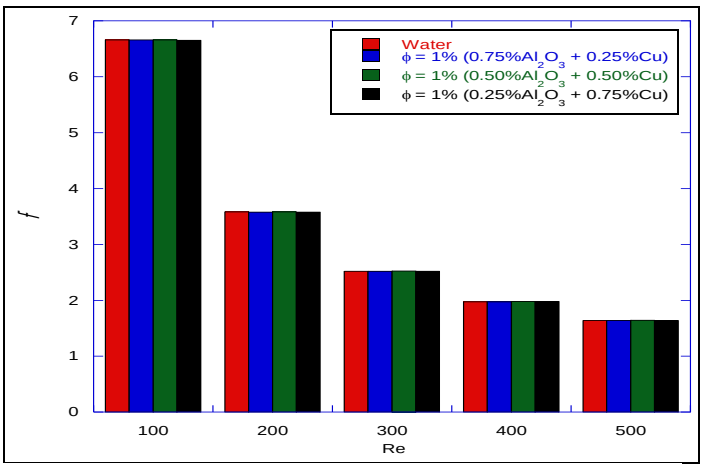

Figure. 6: Effect of Reynolds number on friction factor at fixed hybrid nanoparticle concentration
Source: Authors, (2025).

Furthermore, the friction factor remains relatively consistent at a given Reynolds number, irrespective of the nanoparticle concentration mixed with water. This trend corresponds with the findings from previous studies by Ghale et al [26] and Zhang et al [27]. Specifically, Ghale et al's research, which employed Al_2O_3/Water mixtures in both single and dual-phase setups in ribbed microchannels, indicated that increasing the proportion of particles does not significantly affect the friction factor. Consequently, this suggests that the energy required for pumping the nanofluid remains stable regardless of the Reynolds number.

IV.4 EFFECT OF NANOPARTICLE HYBRIDIZATION ON THE FRICTION FACTOR

Figure 7 demonstrates that an increase in Reynolds number (*Re*) results in a reduction in the friction factor for various concentrations of the hybrid nanofluid. The decline in friction factor, associated with increasing *Re*, is attributed to the dominant effect of inertial forces over the viscous forces in the fluid, as detailed by Lodhi et al [28].

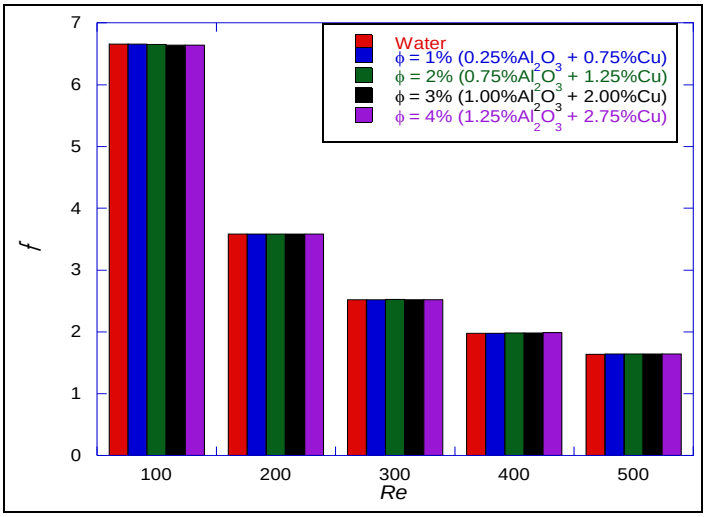

Figure. 7: Effect of Reynolds number on friction factor at diferente hybrid nano particle concentration
Source: Authors, (2025).

Despite these observations, variations in nanoparticle composition appear to have minimal impact on the friction factor, echoing findings by Mohammed et al [29]. This lack of dependency on the friction factor, regardless of changes in the concentration of Al_2O_3 nanoparticles, suggests that the nanofluid behaves similarly to a single-phase fluid, as noted by Byrne et al [30]. A comparable behavior was also observed in the studies by Lee and Mudawar [31], who investigated heat transfer in microchannels using single- and two-phase nanofluids. However, it is generally observed that increasing the concentration of Cu within the mixture enhances the thermal conductivity and heat removal efficiency of the suspension.

IV.5 INFLUENCE OF *RE* ON ENTROPY GENERATION $S'''_{g\text{-}th}$, $S'''_{g\text{-}fr}$, AND $S'''_{g\text{-}total}$

According to Figures 8 and 9, an increase in both *Re* and concentration of Cu in the hybrid nanofluids caused a reduction in $S'''_{g\text{-}th}$ with large deviation at 500 Reynolds number (Figure 8), and $S'''_{g\text{-}total}$ (Figure 9), while $S'''_{g\text{-}fr}$ (Figure 8), increases. The $S'''_{g\text{-}total}$ of the base fluid surpasses that of Al_2O_3/Cu hybrid nanofluid. Mehrali et al [32] utilized a hybrid Fe_3O_4/graphene ferro-nanofluid and

noticed a decrease in entropy generation compared to water. At particle concentrations of 0.25% Cu / 0.75% Al_2O_3, 0.50% Al_2O_3 / 0.50% Cu, and 0.75% Cu / 0.25% Al_2O_3, the value of $S'''_{g\text{-}th}$ in Figure 8 is reduced by 0.86%, 3.16%, and 12.18%, respectively, in comparison to base fluid. While $S'''_{g\text{-}fr}$ in Figure 8 experiences an increase of 10.03%, 8.55%, and 6.67% deviation from the base fluid at particle concentrations of 0.25% Cu / 0.75% Al_2O_3, 0.50% Al_2O_3 / 0.50% Cu, and 0.75% Cu / 0.25% Al_2O_3, respectively.

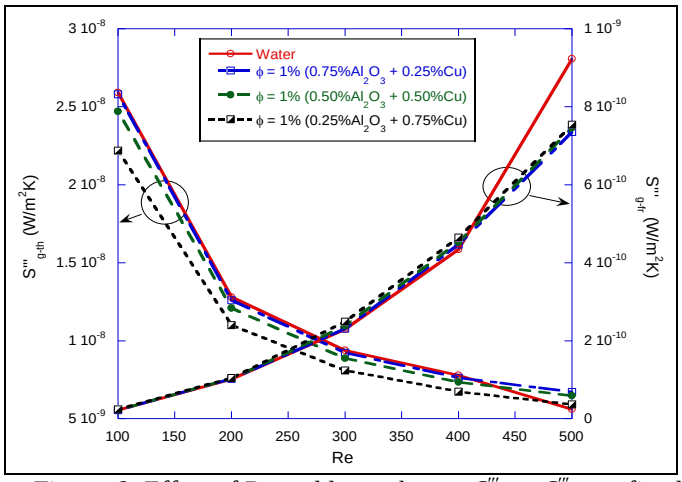

Figure. 8: Effect of Reynolds number on $S'''_{g\text{-}th}$, $S'''_{g\text{-}fr}$ at fixed hybrid nano particle concentration
Source: Authors, (2025).

In Figure 9, the $S'''_{g\text{-}total}$ is reduced by 0.55%, 3.27% and 11.96% at particle concentration of 0.25% Cu / 0.75% Al_2O_3, 0.50% Al_2O_3 / 0.50% Cu and 0.75% Cu / 0.25% Al_2O_3, respectively, compared to the base fluid. These similar trends were observed in the work presented by Saleh and Sundar [33].

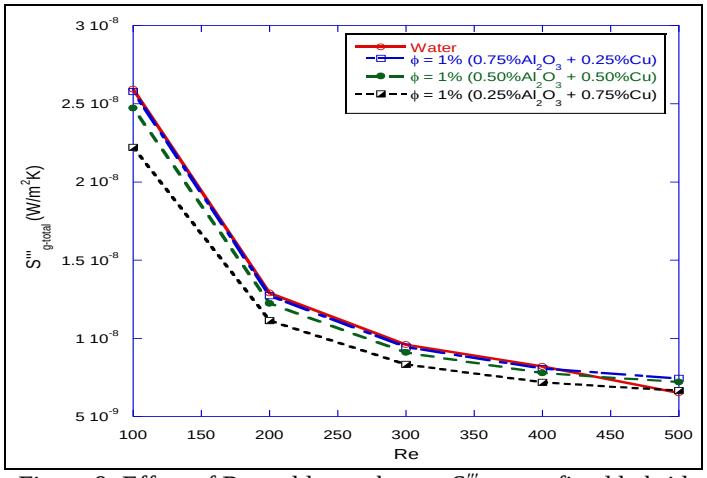

Figure 9: Effect of Reynolds number on $S'''_{g\text{-}total}$ at fixed hybrid nano particle concentration
Source: Authors, (2025).

IV.6 EFFECT OF NANOPARTICLE HYBRIDIZATION ON THE $S'''_{G\text{-}TH}$, $S'''_{G\text{-}FR}$, AND $S'''_{G\text{-}TOTAL}$

Figure 10 illustrates the changes in $S'''_{g\text{-}fr}$ and $S'''_{g\text{-}th}$ as influenced by nanoparticle hybridization. With increasing Reynolds number and nanoparticle concentration, there is an observed rise in $S'''_{g\text{-}fr}$, attributed to the improved thermal conductivity and viscosity of the hybrid nanofluid. Conversely, $S'''_{g\text{-}th}$ decreases with higher Reynolds numbers. These results align with the study by Kanti et al. [34], which investigated heat transfer, entropy generation, and pressure drop using an ash-Cu hybrid nanofluid in tubes. The increase in Reynolds number enhances heat transfer between the fluid and the microchannel wall. Compared to the base fluid, $S'''_{g\text{-}th}$ experienced shifts of 3.27%, 7.71%, 15.98%, and 15.98% for volume fractions of 1%, 2%, 3%, and 4%, respectively. Meanwhile, $S'''_{g\text{-}f}$ showed changes of 6.67%, 5.82%, 5.79%, and 4.76%.

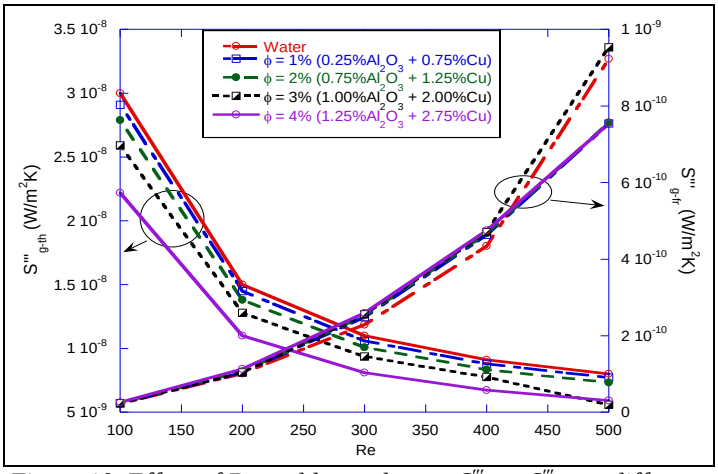

Figure 10: Effect of Reynolds number on $S'''_{g\text{-}th}$, $S'''_{g\text{-}fr}$ at different hybrid nano particle concentration
Source: Authors, (2025).

IV.7 EFFECT OF NANOPARTICLE HYBRIDIZATION ON FIGURE OF MERIT (FOM)

In most methods aimed at enhancing heat transfer, there is a common trade-off: while heat transfer improves, pressure drop also increases. The Figure of Merit (FOM) enables the analysis and comparison of the increment in heat transfer with the energy required to propel the fluid. When FOM >1, this signifies that the thermal efficiency surpasses the energy expended in fluid movement. The impact of hybridization on the FOM becomes evident as the Reynolds number increases. Figure 11 demonstrates that as the average thermal conductivity or fraction of Cu in the hybridized nanofluid rises, the FOM also increases. Specifically, the nanofluid with a concentration of 0.25%Al_2O_3 / 0.75%Cu exhibits a higher effective thermal conductivity compared to the nanofluid with a concentration of 0.5%Al_2O_3 / 0.3%Cu. While they both showed 2.41% and 3.76% shift from 0.75%Al_2O_3 / 0.25%Cu.

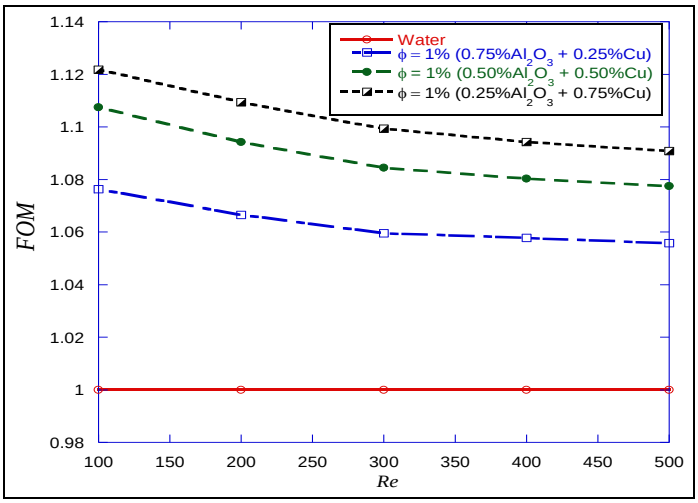

Figure 11: Variation of FOM with Reynolds number at fixed hybrid nanoparticle.
Source: Authors, (2025).

In Figure 12, for a concentration of 4.0% volume, where the copper nanoparticle composition is really high, the maximum FOM corresponds to a *Re* of 100 with 9.10% shift from 1.0% volume of hybrid nanofluid. Conversely, for 1.0% hybrid nanofluid and lower copper concentrations (0.75% volume), the maximum FOM also occurs at a Reynolds number of 100. The lowest FOM is observed at *Re* = 500 for all fractions of hybrid nanofluid. For 1.0% hybrid nanofluid and copper concentrations of 0.75% volume, FOM corresponding to 1.09, while at a value of *Re* = 500, FOM of 1.12 was obtained. However, Kanti et al [34] used fly ash-Cu hybrid nanofluid with Re in turbulent region to obtain similar trends.

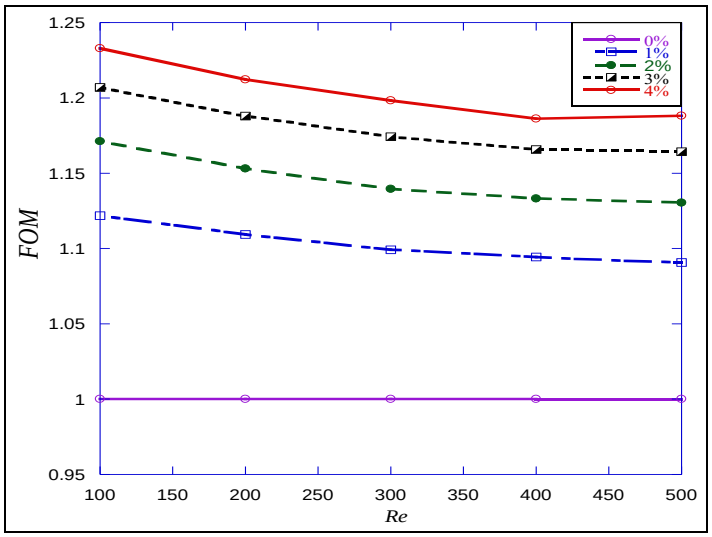

Figure 12: Effect of Reynolds number and hybrid nanoparticle on FOM
Source: Authors, (2025).

V. CONCLUSIONS

This study numerically examined the thermal performance and pressure characteristics of a water-based nanofluid with alumina and copper nanoparticles flowing through a cylindrical microchannel heat sink with internal heat generation at 10^8 W/m³.

The simulation, conducted using ANSYS Fluent computational fluid dynamics software, evaluated the effects of hybridizing copper and alumina nanoparticles on friction factor, Nusselt number, and entropy generation. Parameters included a Reynolds number range of 100 to 500, volume concentrations between 1.0% and 4.0%, and varying proportions of alumina and copper nanoparticles.

Key findings include that increasing the concentration of copper nanoparticles in the hybrid nanofluid did not significantly impact the friction factor. Additionally, thermal and total entropy generation decreased with higher copper concentrations, while Nusselt number and friction entropy generation increased. Notably, increasing both the Reynolds number and copper concentration in the hybrid nanofluids reduced total and thermal entropy generation ($S'''_{g\text{-}th}$), with a deviation observed around Reynolds numbers of 400–500.

In conclusion, the study highlights that the thermal properties of the fluid are critical for designing efficient microchannel heat sinks and confirms the Figure of Merit (FOM) as a valuable tool for performance evaluation.

VI. AUTHOR'S CONTRIBUTION

Conceptualization: Olabode Thomas Olakoyejo, Emmauel Adeyemi, SettingsOlayinka Omowunmi Adewumi, Sogo Mayokun Abolarin, Ibrahim Ademola Fetuga, SettingsAdekunle Omolade Adelaja.
Methodology: Olabode Thomas Olakoyejo, Emmauel Adeyemi, SettingsOlayinka Omowunmi Adewumi, Sogo Mayokun Abolarin, Ibrahim Ademola Fetuga, SettingsAdekunle Omolade Adelaja.
Investigation: Olabode Thomas Olakoyejo, Emmauel Adeyemi, SettingsOlayinka Omowunmi Adewumi, Sogo Mayokun Abolarin, Ibrahim Ademola Fetuga, SettingsAdekunle Omolade Adelaja.
Discussion of results: Olabode Thomas Olakoyejo, Emmauel Adeyemi, SettingsOlayinka Omowunmi Adewumi, Sogo Mayokun Abolarin, Ibrahim Ademola Fetuga, SettingsAdekunle Omolade Adelaja.
Writing – Original Olabode Thomas Olakoyejo, Emmauel Adeyemi, SettingsOlayinka Omowunmi Adewumi, Sogo Mayokun Abolarin, Ibrahim Ademola Fetuga, SettingsAdekunle Omolade Adelaja.
Writing – Review and Editing: Olabode Thomas Olakoyejo, Emmauel Adeyemi, SettingsOlayinka Omowunmi Adewumi, Sogo Mayokun Abolarin, Ibrahim Ademola Fetuga, SettingsAdekunle Omolade Adelaja.
Resources: Olabode Thomas Olakoyejo, Emmauel Adeyemi, SettingsOlayinka Omowunmi Adewumi, Sogo Mayokun Abolarin, Ibrahim Ademola Fetuga, SettingsAdekunle Omolade Adelaja.
Supervision: Olabode Thomas Olakoyejo, Emmauel Adeyemi, SettingsOlayinka Omowunmi Adewumi, Sogo Mayokun Abolarin, Ibrahim Ademola Fetuga, SettingsAdekunle Omolade Adelaja.
Approval of the final text: Olabode Thomas Olakoyejo, Emmauel Adeyemi, SettingsOlayinka Omowunmi Adewumi, Sogo Mayokun Abolarin, Ibrahim Ademola Fetuga, SettingsAdekunle Omolade Adelaja.

VIII. REFERENCES

[1] H. Feng,, J. You, L. Chen, Y. Ge, S. Xia, "Constructal design of a non-uniform heat generating disc based on entropy generation minimization", The European Physical Journal Plus, vol. 135, no. 2, pp. 257, 2020. https://doi.org/10.1140/epjp/s13360-020-00273-3

[2] S. U. Choi, J. A. Eastman, "Enhancing thermal conductivity of fluids with nanoparticles", Argonne National Lab (ANL), (No. ANL/MSD/CP-84938; CONF-951135-29). 1995.

[3] O. T. Olakoyejo, A. O. Adelaja, O. O. Adewumi,A. A. Oluwo, B. K., Bello. S.A. Adio, "Constructal heat transfer and fluid flow enhancement optimisation for cylindrical micro-cooling channels with variable cross-section", Heat Transfer Journal, 50(7), 6757-6775, 2021. https://doi.org/10.1002/htj.22202

[4] V. Kumar, , J. Sarkar "Two-phase numerical simulation of hybrid nanofluid heat transfer in minichannel heat sink and experimental validation", International Communications in Heat and Mass Transfer, vol. 91, pp. 239-247, 2018. https://doi.org/10.1016/j.icheatmasstransfer.2017.12.019

[5] D. Dey, , D. S. Sahu "Nanofluid in the multiphase flow field and heat transfer: A review", Heat Transfer, vol. 50, no. 4, pp. 3722-75. 2021. https://doi.org/10.1002/htj.22050

[6] A. I. Khdair "Numerical simulation of heat transfer of two-phase flow in mini-channel heat sink and investigation the effect of pin-fin shape on flow maldistribution", Engineering Analysis with Boundary Elements, vol. 150, pp. 385-393, 2023. https://doi.org/10.1016/j.enganabound.2023.02.017

[7] A. M. Ali, "Analysis of the heat transfer and flow in minichannel and microchannel heat sinks by single and two-phase mixture models, Doctoral dissertation, University of Leicester, 2023.

[8] M. Faizan, , S. Pati, , P. R. Randive "Implication of geometrical configuration on heat transfer enhancement in converging minichannel using nanofluid by two phase mixture model: A numerical analysis", Proceedings of the Institution of Mechanical Engineers, Part E: Journal of Process Mechanical Engineering, vol. 235, no. 2, pp. 416-427. 2021. https://doi.org/10.1177/0954408920964694

[9] V. Kumar, & J. Sarkar "Numerical and experimental investigations on heat transfer and pressure drop characteristics of Al2O3-TiO2 hybrid nanofluid in minichannel heat sink with different mixture ratio", Powder technology, vol. 345, pp. 717-727. 2019. https://doi.org/10.1016/j.powtec.2019.01.061

[10] H. Upreti, , A. K. Pandey, , M. Kumar "Unsteady squeezing flow of magnetic hybrid nanofluids within parallel plates and entropy generation", Heat Transfer, vol. 50, no. 1, pp. 105-125. 2021. https://doi.org/10.1002/htj.21994

[11] G. Huminic, & A. Huminic "Entropy generation of nanofluid and hybrid nanofluid flow in thermal systems: A review", Journal of Molecular Liquids, vol. 302, 112533. 2020. https://doi.org/10.1016/j.molliq.2020.112533

[12] O. Mahian, , A. Kianifar, , C. Kleinstreuer, , A. N. Moh'd A, , I. Pop, , A. Z. Sahin, , S. Wongwises "A review of entropy generation in nanofluid flow", International Journal of Heat and Mass Transfer, vol. 65, pp. 514-532. 2013. https://doi.org/10.1016/j.ijheatmasstransfer.2013.06.010

[13] R. Nimmagadda, & K. Venkatasubbaiah "Experimental and multiphase analysis of nanofluids on the conjugate performance of micro-channel at low Reynolds numbers", Heat and Mass Transfer, vol. 53, no. 6, pp. 2099-2115. 2017. https://doi.org/10.1007/s00231-017-1970-2

[14] A. A. Alfaryjat, H. A. Mohammed, N. M. Adam, D. Stanciu, & A. Dobrovicescu "Numerical investigation of heat transfer enhancement using various nanofluids in hexagonal microchannel heat sink", Thermal Science and Engineering Progress, vol. 5, pp. 252-262. 2018. https://doi.org/10.1016/j.tsep.2017.12.003.

[15] T. Balaji, C. Selvam, D. M. Lal, & S. Harish "Enhanced heat transport behavior of micro channel heat sink with graphene based nanofluids", International Communications in Heat and Mass Transfer, vol. 117, 104716. 2020. https://doi.org/10.1016/j.icheatmasstransfer.2020.104716

[16] V. M. Krishna, M. S. Kumar, O. Mahesh, & P. S. Kumar "Numerical investigation of heat transfer and pressure drop for cooling of microchannel heat sink using MWCNT-CuO-Water hybrid nanofluid with different mixture ratio", Materials Today: Proceedings, vol. 42, pp. 969-974. 2021. https://doi.org/10.1016/j.matpr.2020.11.935

[17] R. Vinoth, & B. Sachuthananthan "Flow and heat transfer behavior of hybrid nanofluid through microchannel with two different channels", International Communications in Heat and Mass Transfer, vol. 123, 105194. 2021. https://doi.org/10.1016/j.icheatmasstransfer.2021.105194

[18] Y. S. Muzychka "Constructal multi-scale design of compact micro-tube heat sinks and heat exchangers", International journal of thermal sciences, vol. 46(3), pp. 245-252. 2007. https://doi.org/10.1016/j.ijthermalsci.2006.05.002

[19] O. S. Omosehin, A. O. Adelaja, O. T. Olakoyejo, & M. O. Oyekeye "Numerical study of the thermal performance and pressure drops of water-based Al2O3-Cu hybrid nanofluids of different compositions in a microchannel heat sink", Microfluidics and Nanofluidics, vol. 26(49), pp 1-13. 2022. https://doi.org/10.1007/s10404-022-02550-2

[20] M. Kalteh, A. Abbassi, M Safar-Avval, J Harting "Eulerian-Eulerian two-phase numerical simulation of nanofuid laminar forced convection in a microchannel". International Jounal of Heat Fluid Flow 32(1):107– 116. 2011 https://doi.org/10.1016/j.ijheatfuidfow.2010.08.001

[21] A. A. Alfaryjat, D. Stanciu, A. Dobrovicescu, V. Badescu, & M. Aldhaidhawi "Numerical investigation of entropy generation in microchannels heat sink with different shapes", In IOP conference series: materials science and engineering , vol. 147, no. 1, 012134. 2016. IOP Publishing. 10.1088/1757-899X/147/1/012134

[22] A. M. Ali, M. Angelino, & A. Rona "Numerical analysis on the thermal performance of microchannel heat sinks with Al2O3 nanofluid and various fins", Applied Thermal Engineering, vol.198, 117458. 2021. https://doi.org/10.1016/j.applthermaleng.2021.117458

[23] Z. Azizi, A. Alamdari, & M. R. Malayeri "Convective heat transfer of Cu–water nanofluid in a cylindrical microchannel heat sink", Energy Conversion and Management, vol. 101, pp. 515-524. 2015. https://doi.org/10.1016/j.enconman.2015.05.073

[24] L. Zheng, Y. Xie, & D. Zhang "Numerical investigation on heat transfer performance and flow characteristics in circular tubes with dimpled twisted tapes using Al2O3-water nanofluid", International Journal of Heat and Mass Transfer, vol. 111, pp. 962-981. 2017. https://doi.org/10.1016/j.ijheatmasstransfer.2017.04.062

[25] M. Ataei, , F. S. Moghanlou, , S. Noorzadeh, , M. Vajdi, , M. S. Asl "Heat transfer and flow characteristics of hybrid Al2O3/TiO2 – water nanofluid in a minichannel heat sink", Heat and Mass Transfer, vol. 56, pp. 2757-2767. 2020. https://doi.org/10.1007/s00231-020-02896-9

[26] Z. Y. Ghale, , M. Haghshenasfard, , M. N. Esfahany "Investigation of nanofluids heat transfer in a ribbed microchannel heat sink using single-phase and multiphase CFD models", International Communications in Heat and Mass Transfer, vol. 68, pp. 122-129. 2015. https://doi.org/10.1016/j.icheatmasstransfer.2015.08.012

[27] X. Zhang, , R. C. Li, , Q. Zheng "Analysis and simulation of high-power LED array with microchannel heat sink. Advances in Manufacturing", vol. 1, pp. 191-195. 2013. https://doi.org/10.1007/s40436-013-0027-0

[28] M. S. Lodhi, , T. Sheorey, , G. Dutta "Single-phase fluid flow and heat transfer characteristics of nanofluid in a circular microchannel: Development of flow and heat transfer correlations", Proceedings of the Institution of Mechanical Engineers, Part C: Journal of Mechanical Engineering Science, vol. 234, no. 18, pp. 3689-3708. 2020. https://doi.org/10.1177/0954406220916537

[29] H. A. Mohammed, , P. Gunnasegaran, , N. H. Shuaib "The impact of various nanofluid types on triangular microchannels heat sink cooling performance", International Communications in Heat and Mass Transfer, vol. 38, no. 6, pp. 767-773. 2011. https://doi.org/10.1016/j.icheatmasstransfer.2011.03.024

[30] M. D. Byrne, , R. A. Hart, , A. K. Da Silva "Experimental thermal–hydraulic evaluation of CuO nanofluids in microchannels at various concentrations with and without suspension enhancers", International Journal of Heat and Mass Transfer, vol. 55, no. 9, pp. 2684-2691. https://doi.org/10.1016/j.ijheatmasstransfer.2011.12.018

[31] J. Lee, , & I. Mudawar, I "Assessment of the effectiveness of nanofluids for single-phase and two-phase heat transfer in micro-channels", International Journal of Heat and Mass Transfer, vol. 50, no. 3-4, pp. 452-463. 2007. https://doi.org/10.1016/j.ijheatmasstransfer.2011.12.018

[32] M. Mehrali, , E. Sadeghinezhad, , A. R. Akhiani, , S. T. Latibari, , H. S. C. Metselaar, , A. S. Kherbeet, , M. Mehrali "Heat transfer and entropy generation analysis of hybrid graphene/Fe3O4 ferro-nanofluid flow under the influence of a magnetic field" Powder technology, vol. 308, pp. 149-157. 2017. https://doi.org/10.1016/j.powtec.2016.12.024

[33] B. Saleh, & L. S. Sundar "Entropy generation and exergy efficiency analysis of ethylene glycol-water based nanodiamond+ Fe3O4 hybrid nanofluids in a circular tube. Powder Technology, vol. 380, pp. 430-442. 2021. https://doi.org/10.1016/j.powtec.2020.12.006

[34] P. K. Kanti, , K. V. Sharma, , A. A. Minea, , V. Kesti "Experimental and computational determination of heat transfer, entropy generation and pressure drop under turbulent flow in a tube with fly ash-Cu hybrid nanofluid", International Journal of Thermal Sciences, vol. 167, 107016. 2021. https://doi.org/10.1016/j.ijthermalsci.2021.107016